DRAFT VERSION MAY 25, 2015
Preprint typeset using LaTeX style emulateapj v. 12/16/11

DISCOVERY OF MASSIVE, MOSTLY STAR-FORMATION QUENCHED GALAXIES WITH EXTREMELY STRONG LYMAN α EMISSION AT $Z \sim 3$*

YOSHIAKI TANIGUCHI[1], MASARU KAJISAWA[1,2], MASAKAZU A. R. KOBAYASHI[1], TOHRU NAGAO[1], YASUHIRO SHIOYA[1], NICK Z. SCOVILLE[3], DAVID B. SANDERS[4], PETER L. CAPAK[3,5], ANTON M. KOEKEMOER[6], HENRY J. MCCRACKEN[7], OLIVIER LE FÈVRE[8], LIDIA TASCA[8], KARTIK SHETH[9], ALVIO RENZINI[10], SIMON LILLY[11], MARCELLA CAROLLO[11], KATARINA KOVAČ[11], OLIVIER ILBERT[8], EVA SCHINNERER[12], HAI FU[13], SUNE TOFT[14], AND LAURENCE TRESSE[15]

Draft version May 25, 2015

ABSTRACT

We report a discovery of 9 massive galaxies with both extremely large Lyα equivalent width and evolved stellar population at $z \sim 3$. These MAssive Extremely STrong Lyα emitting Objects (MAESTLOs) have been discovered in our large-volume systematic survey for strong Lyα emitters (LAEs) with twelve intermediate-bands data taken with Subaru/Suprime-Cam in the COSMOS field. Based on the SED fitting analysis for these LAEs, it is found that these MAESTLOs have (1) large rest-frame equivalent width of $EW_0(\mathrm{Ly}\alpha) \sim 100$–$300$ Å, (2) $M_\star \sim 10^{10.5}$–$10^{11.7}$ $M_\odot$, and (3) relatively low specific star formation rates of $SFR/M_\star \sim 0.03$–1 Gyr^{-1}. They have extended Lyα emission although they show compact morphology in the HST/ACS images, which correspond to the rest-frame UV continuum. It is also found that most of the MAESTLOs do not show any evidence for AGNs in the VLA, XMM, and Spitzer data, while the two most massive MAESTLOs are detected in the Chandra data. We suggest that these new class of LAEs provide a possible missing link from star-forming to passively evolving galaxies at the peak era of the cosmic star-formation history.

Keywords: cosmology: observations — early universe — galaxies: formation — galaxies: evolution — galaxies: high-redshift

1. INTRODUCTION

Most of massive galaxies in the present universe are passively evolving galaxies with little on-going star formation (e.g., Kauffmann et al. 2003). In the current understanding of galaxy evolution, massive galaxies are considered to have evolved more rapidly than less massive systems in earlier universe: so-called the downsizing evolution of galaxies (Cowie et al. 1996). These massive galaxies have formed their stars actively by a cosmic age of a few Gyr (redshift $z \sim 2$–3), when the cosmic star formation rate density peaked (e.g., Bouwens et al. 2011). After this epoch, their star formation stopped and they passively evolved into elliptical galaxies seen today. However, the quenching mechanism of star formation in these massive galaxies has not yet been understood because the process may have occurred in a relatively short time scale, making it difficult to observe such events (e.g., Renzini et al. 2009; Peng et al. 2010; Durkalec et al. 2015; Mancini et al. 2015).

Among various possible methods, star-forming activity in galaxies is probed by their strong emission lines such as Hydrogen recombination and/or metallic lines. To seek for star-forming galaxies in young universe, the Hydrogen Lyα emission provides the most useful tool. Therefore, many searches for redshifted Lyα emission have resulted in the discovery of young galaxies beyond $z \sim 7$, corresponding to an cosmic age of $\lesssim 750$ Myr (Ono et al. 2012; Shibuya et al. 2012; Finkelstein et al. 2013; Konno et al. 2014; Schenker et al. 2014). Among such Lyα emitting galaxies (Lyα emitters, hereafter LAEs), those with a very large equivalent width (EW), i.e., extremely strong LAEs, are particularly important in that they can be galaxies in a very early stage of galaxy formation (e.g., Schaerer 2003; Nagao et al. 2007).

In order to search for them, we have carried out a survey for extremely strong LAEs over an unprecedentedly large volume. While most of the detected objects with strong Lyα seem to be young galaxies with small stellar mass as expected for LAEs, we have serendipitously found 9 massive galaxies with extremely large $EW(\mathrm{Ly}\alpha)$ and relatively evolved stellar population at $z \sim 3$. Here we present the physical properties

tani@cosmos.phys.sci.ehime-u.ac.jp

* Based on observations with NASA/ESA *Hubble Space Telescope*, obtained at the Space Telescope Science Institute, which is operated by AURA, Inc., under NASA contract NAS 5-26555; and also based on data collected at Subaru Telescope, which is operated by the National Astronomical Observatory of Japan; and also based on data products from observations made with ESO Telescopes at the La Silla Paranal Observatory under ESO programme ID 179.A-2005 and on data products produced by TERAPIX and the Cambridge Astronomy Survey Unit on behalf of the UltraVISTA consortium.

[1] Research Center for Space and Cosmic Evolution, Ehime University, Bunkyo-cho, Matsuyama 790-8577, Japan
[2] Graduate School of Science and Engineering, Ehime University, Bunkyo-cho, Matsuyama 790-8577, Japan
[3] Department of Astronomy, MS 105-24, California Institute of Technology, Pasadena, CA 91125, USA
[4] Institute for Astronomy, University of Hawaii, 2680 Woodlawn Drive, Honolulu, HI 96822, USA
[5] Spitzer Science Center, California Institute of Technology, Pasadena, CA 91125, USA
[6] Space Telescope Science Institute, 3700 San Martin Drive, Baltimore, MD 21218, USA
[7] Institut d'Astrophysique de Paris, UMR7095 CNRS, Université Pierre et Marie Curie, 98 bis Boulevard Arago, 75014, Paris, France
[8] Aix Marseille Université, CNRS, LAM (Laboratoire d'Astrophysique de Marseille), UMR 7326, 13388, Marseille, France
[9] National Radio Astronomy Observatory, 520 Edgemont Road, Charlottesville, VA 22903, USA
[10] Dipartimento di Astronomia, Universita di Padova, vicolo dell'Osservatorio 2, 35122, Padua, Italy
[11] Department of Physics, ETH Zurich, 8093, Zurich, Switzerland
[12] MPI for Astronomy, Königstuhl 17, D-69117 Heidelberg, Germany
[13] Department of Physics & Astronomy, University of Iowa, Iowa City, IA 52245, USA
[14] Dark Cosmology Centre, Niels Bohr Institute, University of Copenhagen, Juliane Mariesvej 30, DK-2100 Copenhagen, Denmark
[15] Laboratoire d'Astrophysique de Marseille (UMR 6110), CNRS-Université de Provence, BP 8, 13376 Marseille Cedex 12, France

Table 1
Physical Properties of the 9 MAESTLOs

No.	$z_{\rm phot}$	$\log M_\star$	τ	age	$E(B-V)$	$EW_0({\rm Ly}\alpha)$	$\log[SFR/(M_\odot\ {\rm yr}^{-1})]$		Half Light Radius $r_{\rm HL}$ (kpc)		
		($M_\odot$)	(Gyr)	(Gyr)	(mag)	(Å)	Lyα	SED	ACS F814W	S-Cam i'	S-Cam IA
1	3.07[a]	$11.72^{+0.02}_{-0.01}$	$0.79^{+0.21}_{-0.00}$	$1.80^{+0.20}_{-0.12}$	$0.30^{+0.03}_{-0.03}$	115 ± 7	$1.21^{+0.02}_{-0.02}$	$2.12^{+0.14}_{-0.12}$	5.43 ± 0.18	6.97 ± 0.08	12.56 ± 0.07
2	2.99	$11.51^{+0.02}_{-0.39}$	$1.26^{+0.33}_{-1.20}$	$2.10^{+0.00}_{-1.85}$	$0.46^{+0.08}_{-0.03}$	193^{+37}_{-19}	$0.61^{+0.04}_{-0.05}$	$2.01^{+0.33}_{-0.37}$	0.60 ± 0.12	6.17 ± 0.21	19.99 ± 0.48
3	2.99	$11.33^{+0.01}_{-0.10}$	$0.50^{+0.00}_{-0.25}$	$2.10^{+0.00}_{-0.82}$	$0.22^{+0.02}_{-0.11}$	188^{+26}_{-42}	$0.68^{+0.04}_{-0.04}$	$1.07^{+0.08}_{-0.37}$	—[d]	—[g]	4.46 ± 0.19
4	3.16	$11.11^{+0.08}_{-0.00}$	$0.32^{+0.08}_{-0.00}$	$1.61^{+0.29}_{-0.18}$	$0.03^{+0.06}_{-0.00}$	240^{+20}_{-19}	$1.12^{+0.02}_{-0.02}$	$0.63^{+0.26}_{-0.00}$	0.52 ± 0.05	<3.87[f]	4.50 ± 0.07
5	2.81	$11.11^{+0.04}_{-0.07}$	$1.59^{+1.58}_{-0.59}$	$1.80^{+0.40}_{-0.52}$	$0.29^{+0.03}_{-0.02}$	306 ± 20	$1.20^{+0.02}_{-0.02}$	$1.79^{+0.12}_{-0.08}$	—[e]	4.49 ± 0.09	6.68 ± 0.09
6	2.81[b]	$10.90^{+0.00}_{-0.00}$	$0.05^{+0.00}_{-0.00}$	$0.29^{+0.00}_{-0.00}$	$0.19^{+0.00}_{-0.00}$	171 ± 6	$1.04^{+0.02}_{-0.02}$	$0.89^{+0.00}_{-0.00}$	1.00 ± 0.04	4.21 ± 0.09	7.18 ± 0.18
7	3.24	$10.71^{+0.12}_{-0.03}$	$0.40^{+0.40}_{-0.00}$	$1.28^{+0.62}_{-0.14}$	$0.12^{+0.05}_{-0.04}$	110 ± 15	$0.70^{+0.05}_{-0.05}$	$0.94^{+0.22}_{-0.16}$	0.34 ± 0.02	<3.83[f]	<5.70[f]
8	2.50[c]	$10.54^{+0.08}_{-0.04}$	$0.06^{+9.94}_{-0.02}$	$0.14^{+0.26}_{-0.03}$	$0.40^{+0.04}_{-0.03}$	107^{+11}_{-14}	$0.68^{+0.03}_{-0.03}$	$1.94^{+0.37}_{-0.27}$	<0.57[f]	<4.12[f]	3.77 ± 0.12
9	3.16	$10.52^{+0.03}_{-0.03}$	$0.50^{+0.00}_{-0.00}$	$1.90^{+0.00}_{-0.10}$	$0.02^{+0.02}_{-0.01}$	124 ± 16	$0.64^{+0.05}_{-0.05}$	$0.41^{+0.08}_{-0.03}$	<0.54[f]	<3.87[f]	<5.74[f]

Note. — The No. is given in order of decreasing the estimated stellar mass. Errors for $\log M_\star$, τ, age, $E(B-V)$, $EW_0({\rm Ly}\alpha)$, $\log SFR({\rm Ly}\alpha)$, and $\log SFR({\rm SED})$ correspond to 1-σ confidence interval (i.e., $\Delta\chi^2\leq1$) estimated from the SED fitting. In the SED fitting, the templates older than cosmic age at $z_{\rm phot}$ are not used. The entry of 0.00 for these errors indicate that there is no parameter grid in $\Delta\chi^2\leq1$ around the best-fit model parameter.

[a] $z_{\rm spec}=3.086$.
[b] $z_{\rm spec}=2.798$.
[c] $z_{\rm spec}=2.513$.
[d] Undetected.
[e] Out of the ACS/F814W-band data.
[f] Unresolved.
[g] Cannot fitted by Sérsic law.

of this new population expected to be in a transition phase between active star-forming and passive evolution. In this paper, we use a standard cosmology with $\Omega_M=0.3$, $\Omega_\Lambda=0.7$, and $H_0=70$ km s^{-1} Mpc^{-1}.

2. DATA AND ANALYSIS

In this study, we use the multi-wavelength data set from the Cosmic Evolution Survey (COSMOS; Scoville et al. 2007). Optical imaging data with 12 intermediate-band (hereafter, IA-band) filters equipped on Subaru/Suprime-Cam allow us to pick up strong emission-line objects by a significant flux excess in one of the IA bands. The spectral resolution of our IA filters is $R=\lambda/\Delta\lambda=$ 20–26, and the 12 IA filters cover the whole optical wavelength range from 4270 Å to 8270 Å (Taniguchi et al. 2015). Therefore, we can search for strong LAEs at $2.5<z<5.8$. Although the details of our selection procedure for strong LAEs are given elsewhere (Kobayashi et al., in prep.), we briefly summarize it in the following.

At first, from the COSMOS Official Photometric Catalog (version 2012, Capak et al. 2007), we selected objects with a significant (3σ) flux excess in an IA band from the frequency-matched continuum estimated by using two adjacent broad-band magnitudes. In order to identify which emission line causes the IA-band excess of these objects, we applied the public photometric redshift code EAZY (Brammer et al. 2008) to the multi-band photometric data from optical to MIR, which include CFHT u^* and i^*, Subaru $Bg'Vr'i'z'$ and 12 IA bands (Taniguchi et al. 2007), UltraVISTA $YJHK$ (McCracken et al. 2012), and Spitzer/IRAC 3.6 μm and 4.5 μm bands (Sanders et al. 2007). The excess IA band and any broad bands whose wavelength coverage is overlapped with the excess IA band are excluded from the photometric redshift calculation. We adopted a line identification with the highest probability in the volume-weighted redshift likelihood function, and assigned the photometric redshift assuming the emission line enters into the effective wavelength of the excess IA band. We selected LAEs from these strong emission-line objects and then performed the spectral energy distribution (SED) fitting with the GALAXEV population synthesis model (Bruzual & Charlot 2003) to estimate the physical properties of the LAEs. In the SED fitting, we assumed the exponentially decaying star formation histories with an e-folding timescale of $\tau=0.01$–10 Gyr. The Chabrier initial mass function (Chabrier 2003) and the Calzetti extinction law (Calzetti et al. 2000) were adopted. In addition to the multi-band photometry used in the photometric redshift estimate, we also used the IRAC 5.8 μm and 8.0 μm bands to obtain more accurate physical properties such as the stellar mass and age. Our survey covers a 1.34 square degree area in the COSMOS field, that is, the overlapped area between COSMOS deep region and UltraVISTA DR1 (McCraken et al. 2012). The wide survey area and wide wavelength coverage of the 12 IA bands allow us to search strong LAEs at $2.5<z<5.8$ over a very large volume of 5.5×10^7 Mpc^3.

Since our main interest is the star-forming activity in galaxies, we rejected possible active galactic nuclei (AGN) by using the IRAC color criteria proposed by Donley et al. (2012). We also used both the XMM-COSMOS (Hasinger et al. 2007) and VLA-COSMOS (Schinnerer et al. 2007) catalogues to reject AGNs; note that the sensitivity for the VLA data is 10.5–15 μJy/beam and that for the XMM data is 5×10^{-16} erg s^{-1} cm^{-2}. After excluding 30 objects from the sample as AGNs, we finally obtained 525 non-AGN LAEs at $z\sim2.5$–4.6. In this sample, 65 LAEs show an extremely large rest-frame equivalent width of $EW_0({\rm Ly}\alpha)\geq100$ Å. Among them, 9 LAEs turn out to be extremely strong LAEs are massive galaxies at $2.5<z<3.2$ which have a stellar mass with $M_\star\geq10^{10.5}\ M_\odot$ (see Table 1). Hereafter, we call these 9 LAEs MAssive, Extremely STrong Lyα emitting Objects (MAESTLOs).

Their sizes are measured in the excess IA-band (i.e., Lyα image) and the COSMOS HST/ACS $I_{\rm F814W}$-band mosaics (Koekemoer et al. 2007), corresponding to the rest-frame UV

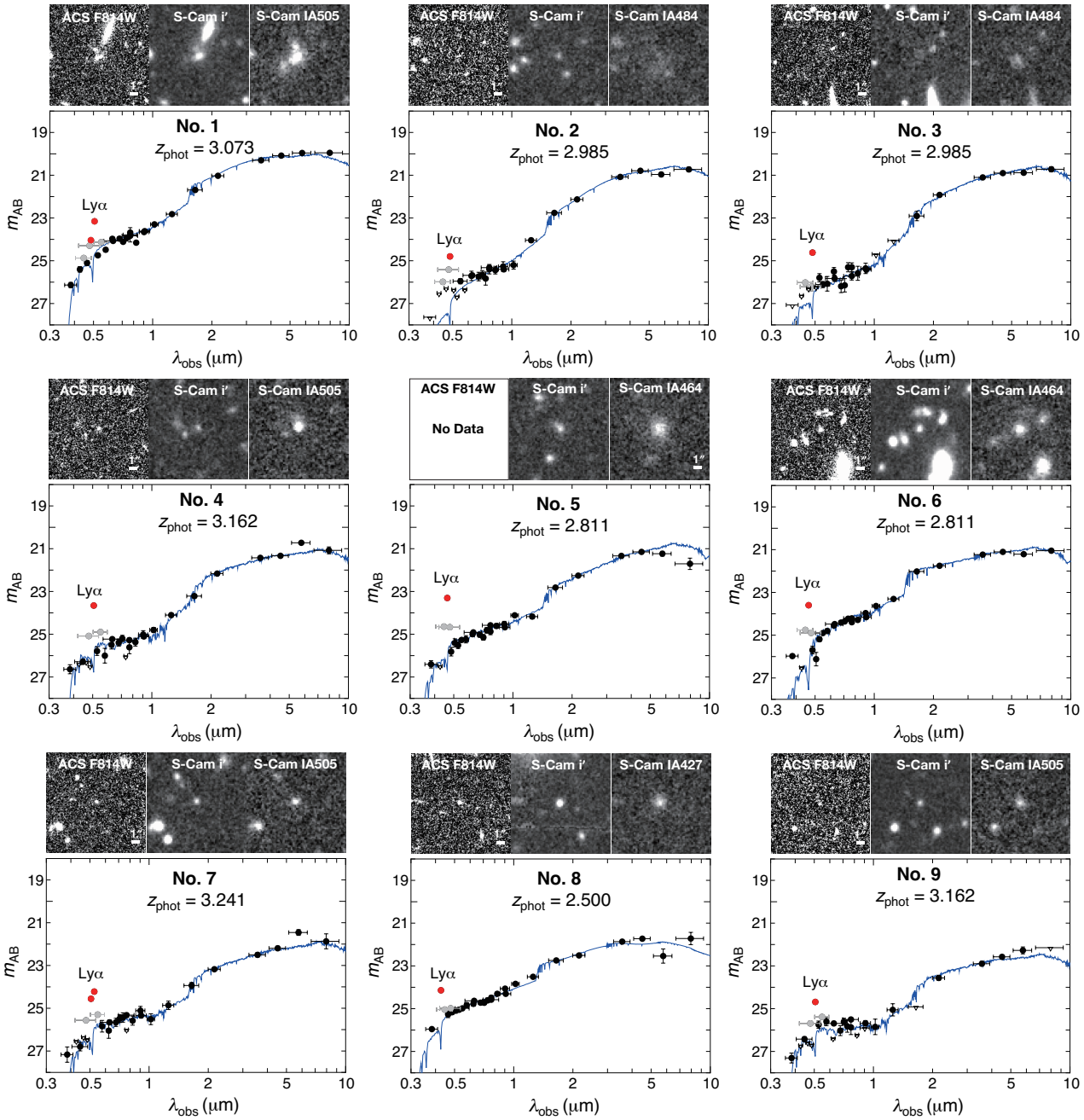

Figure 1. SEDs and HST and Subaru images of the 9 MAESTLOs. In the bottom main panel, the observed data points are shown by filled circles with error bars. The red symbol shows the IA band with a significant flux excess by the Lyα emission, while the grey symbols represent the broad bands whose wavelength coverage overlaps with the excess IA band. The blue curve shows the best-fit model SED from the GALAXEV library. The data affected by the strong Lyα emission (red and grey points) are not used in the SED fitting. The inverted triangles represents the 3σ upper limit for the undetected bands. In the top panels, the thumbnails of the HST ACS in the F814W filter, the Subaru Suprime-Cam i'-band image, and the excess IA-band image are shown. Each panel is $12'' \times 12''$ in size. The ACS images are convolved with a Gaussian kernel with $\sigma = 1$ pix ($= 0.03''$) to reduce the noise.

continuum, by using the GALFIT code (Peng et al. 2002). We fit the observed surface brightness with an exponential law, taking account of the point spread function (PSF) of these data. The PSF images of the excess IA-band and ACS data are measured by combining relatively bright isolated stars in each image. Note, however, that we cannot measure the ACS sizes for the following two MAESTLOs; (1) No. 3 is not detected in the ACS image because of its faint surface brightness and (2) No. 5 is out of the HST/ACS filed. Furthermore, we also checked the sizes of the rest-frame UV continuum using the i'-band data taken with the same instrument as the excess IA-band data. The estimated half-light radii of the MAESTLOs are shown in Table 1.

3. RESULTS & DISCUSSIONS

In Figure 1, we show the rest-frame UV–NIR SED of the 9 MAESTLOs together with their thumbnails in the excess IA, i', and ACS $I_{\rm F814W}$ bands. It is found that they are significantly bright in the rest-frame NIR wavelength, leading to their large estimated stellar masses of $\log(M_\star/M_\odot) = 10.5$–$11.7$. Another unexpected property is that they show very red rest-frame UV-optical colors despite of their extremely strong

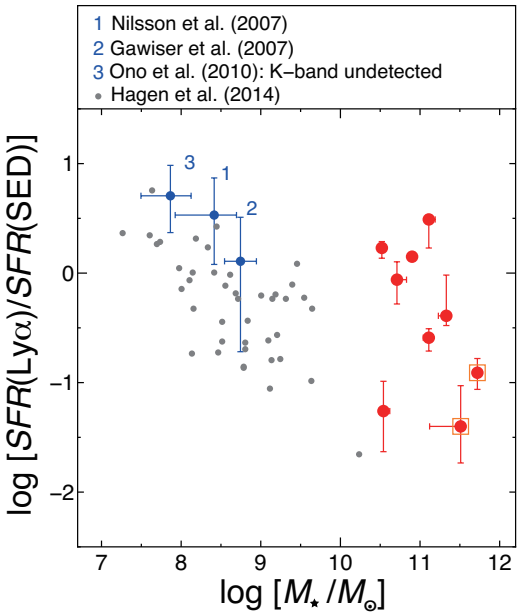

Figure 2. $SFR(\mathrm{Ly}\alpha)/SFR(\mathrm{SED})$ vs. $M_\star$ for our MAESTLOs (filled red circles) and LAEs at $z \sim 3$ from the literatures (filled blue circles for the results from stacked LAEs and filled gray circles for those from individual LAE). For Hagen et al. (2014), we plot only the LAEs at $z = 2.5$–3.5 in their sample. Note that the SFRs in the literatures derived with the Salpeter IMF are converted into those with the Chabrier IMF we use. Note also that Hagen et al. (2014) used the SFRs estimated from the dust-corrected UV luminosity instead of those based on the SED fitting. The two MAESTLOs detected with Chandra are shown with open orange boxes.

Lyα emission; i.e., the MAESTLOs show a relatively strong 4000 Å continuum break in the rest-frame optical as well as the Lyman break in the rest-frame far-UV. These continuum features allow us to identify the flux excess in a concerned IA band as the Lyα emission line, resulting in an accurate photometric redshift for them. In fact, three of the 9 MAESTLOs have spectroscopic identifications and their spectroscopic redshifts agree with the photometric redshifts estimated from the IA-band excess (Nos. 1, 6, and 8; see Table 1). The strong 4000 Å break observed in the MAESTLOs suggests relatively old stellar population in them, and their best-fit stellar ages based on SED fitting are 1–2 Gyr[17]. Thus these galaxies form a completely different population from typical high-redshift LAEs with both a small stellar mass and a young stellar age (e.g., Ono et al. 2010; Hagen et al. 2014).

Despite their relatively old stellar population, the MAESTLOs have extremely large rest-frame equivalent widths of $EW_0(\mathrm{Ly}\alpha) \sim 100$–$300$ Å. In order to compare the star formation rates (SFR) estimated from Lyα luminosity, $SFR(\mathrm{Ly}\alpha)$, with that from SED fitting, $SFR(\mathrm{SED})$, we show $SFR(\mathrm{Ly}\alpha)/SFR(\mathrm{SED})$ ratios of the MAESTLOs as a function of stellar mass in Figure 2. Here, we use the Kennicutt (1998) relation between SFR and $L(\mathrm{H}\alpha)$ combined with both the $L(\mathrm{Ly}\alpha)/L(\mathrm{H}\alpha)$ ratio of 8.7 under the case B recombination and a correction factor converting from the Salpeter IMF into the Chabrier IMF (i.e., multiplied by a factor of 0.60). For typical LAEs, it is found that the $SFR(\mathrm{Ly}\alpha)/SFR(\mathrm{SED})$ ratio decreases with increasing stellar mass (Hagen et al. 2014). On the other hand, for most MAESTLOs, $SFR(\mathrm{Ly}\alpha)$ is comparable to $SFR(\mathrm{SED})$ and thus their $SFR(\mathrm{Ly}\alpha)/SFR(\mathrm{SED})$ ratios are similar to those of typical LAEs with much smaller masses. Therefore, it is suggested that the escape fraction of the Lyα emission is relatively high in these galaxies and/or that there are other additional energy sources besides the photoionization by massive OB stars. We infer that the observed extremely strong Lyα emission is attributed to a large-scale superwind surrounding the MAESTLOs. The shock heating associated with the outflowing gas can produce the additional Lyα emission because such supernova-driven shocks can provide a significantly high Lyα luminosity, which is comparable to the photoionization by young massive stars (e.g., Mori & Umemura 2006). Furthermore, if the high-velocity gas outflows are induced by supernova feedback, a large fraction of Lyα photons in these MAESTLOs can escape from the galaxy itself (e.g., Kunth et al. 1998). Indeed, the size of MAESTLOs in the IA-band images (i.e., the Lyα images) is systematically larger than that in the HST ACS ones (rest-frame UV continuum image); the half-light radius in the IA-band data is $\sim$ 4–20 kpc, while that in the ACS data is $\sim$ 0.3–0.9 kpc except for the most massive MAESTLO (Figure 3). Even if we use the Subaru/Suprime-Cam i'-band data for the rest-frame UV continuum instead of the ACS data and compare the sizes between the data taken with the same instrument, the size in the excess IA-band image is systematically larger than that in the i'-band image (Table 1). Therefore, the observed extended Lyα emission in the MAESTLOs can mostly be attributed to superwind-driven outflows.

Another possibility for such extended emission-line regions is jets and/or outflows from AGN. Although we already excluded AGNs from our sample in the selection procedures with the IRAC colors and the XMM and VLA data as mentioned above, we carried out additional checks for the AGN possibility with the Spitzer/MIPS 24 μm and Chandra X-ray data. We found that none of the MAESTLOs has a MIPS 24 μm counterpart with $f_{24\mu\mathrm{m}} > 0.15$ mJy (Sanders et al. 2007), where hot dust grains in a dusty torus around the central engine of an AGN could emit strong mid-infrared emission. On the other hand, the two most massive MAESTLOs (Nos. 1 and 2) are detected in the Chandra data from the C-COSMOS survey (Elvis et al. 2009), which covers a 0.9 deg^2 region of the COSMOS field and 7 out of the 9 MAESTLOs. Note that five MAESTLOs are not detected and the remaining two are out of the Chandra survey area. While the detection of MAESTLO No. 1 is marginal ($1.8 \pm 0.7 \times 10^{-15}$ erg s^{-1} cm^{-2} in the full band and $2.9 \pm 1.3 \times 10^{-15}$ erg s^{-1} cm^{-2} in the hard band), MAESTLO No. 2 is significantly detected in both of the full ($3.9 \pm 0.6 \times 10^{-15}$ erg s^{-1} cm^{-2}) and soft ($1.0 \pm 0.2 \times 10^{-15}$ erg s^{-1} cm^{-2}) bands. Therefore, these two MAESTLOs possibly host AGNs and the relatively large size of their Lyα emission (Figure 3) may be attributed to AGN phenomena such as outflows or extended narrow-line regions (e.g., Schirmer et al. 2013). Note, however, that there is little evidence for non thermal continuum in their rest-frame UV-to-NIR SEDs. Although the other MAESTLOs do not show any evidence for AGNs, we cannot completely rejected the possibility of weak AGN for these objects because of the limited depths of the IRAC, MIPS 24 μm, X-ray, and radio data. It is also possible that these objects would be AGNs that have just died, but the extended line emission still remains.

[17] Note that 2 MAESTLOs (i.e., Nos. 6 and 8) have relatively young ages. No. 6 has a very short e-folding timescale and a clear Balmer break in the SED, suggesting that its SFR is rapidly decreasing. On the other hand, No. 8 shows relatively weak Balmer/4000 Å break compared to the other MAESTLOs and its e-folding timescale is highly uncertain.

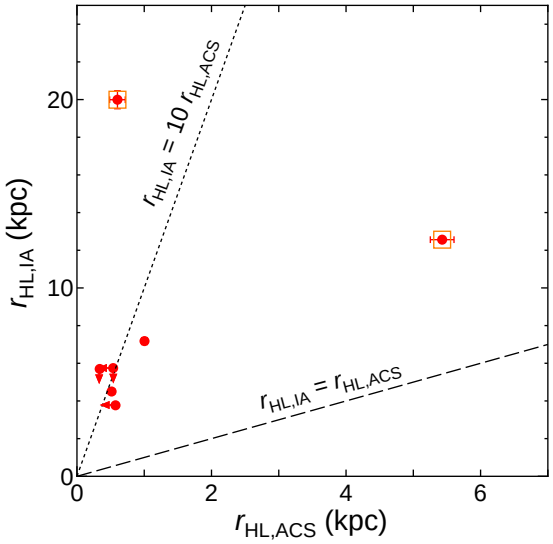

Figure 3. Comparison between the half-light radius r_{HL} in the IA-band data (Lyα image) and that in the HST/ACS data (rest-frame UV continuum image) for MAESTLOs. The arrows indicate upper limit of r_{HL} for the MAESTLOs unresolved in the IA-band and/or HST/ACS data. Note that the error in both radii is typically smaller than the symbol size except for the 1st and 2nd most massive MAESTLOs. Since one MAESTLO is undetected (No. 3) and another is out of the ACS/F814W-band field (No. 5), they are not shown in this plot. The two MAESTLOs detected with Chandra are shown with open orange boxes.

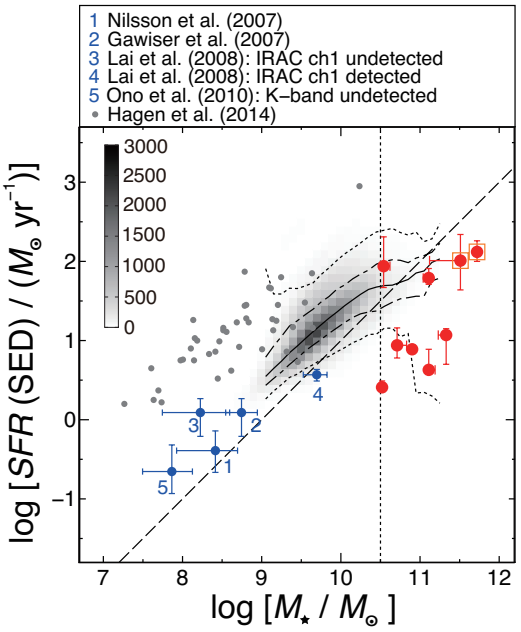

Figure 4. SFR(SED) vs. $M_\star$ for the same samples as shown in Figure 2 and for the LAE samples at $z \sim 3.1$ detected and undetected in IRAC 3.6 μm band. Our MAESTLOs are shown as filled red circles and LAEs from the literatures are shown as filled blue circles and filled gray circles in the same manner as that in Figure 2. Note that SFR(SED) and $M_\star$ in the literatures derived with the Salpeter IMF are converted into those with the Chabrier IMF we use. We plot the so-called main sequence of star-forming galaxies at $z_{phot} = 2.5$–3.5 in the COSMOS field in gray scale with bin size of 0.1 dex in $M_\star$ and SFR. The scale (the number of galaxies per bin) is shown in the upper-left inset. Solid line, dot-dashed lines, and dotted lines show the median, 16 and 84 percentiles, and 2.5 and 97.5 percentiles in bins of 0.1 dex in stellar mass. The dashed line shows the relation of $sSFR = 1$ Gyr^{-1}. The vertical dotted line corresponds to $\log(M_\star/M_\odot) = 10.5$, which is one of the criteria of MAESTLO.

In order to investigate their evolutionary stage, we show the distribution of MAESTLOs in the SFR(SED)–$M_\star$ plane together with typical LAEs at $z \sim 3$ (Nilsson et al. 2007; Gawiser et al. 2007; Lai et al. 2008; Ono et al. 2010; Hagen et al. 2014) and galaxies at $z_{phot} = 2.5$–3.5 in the COSMOS field (Figure 4). Compared to normal star-forming galaxies on the main sequence at similar stellar masses and redshifts, the MAESTLOs have a smaller specific SFR, $sSFR = SFR/M_\star \sim 0.03$–$1$ Gyr^{-1}, suggesting that their star formation activities are just ceasing and that they are in a transition phase from actively star-forming galaxies into quiescent galaxies. This contrasts with normal LAEs that tend to have a sSFR similar with or higher than main-sequence galaxies (e.g., Hagen et al. 2014). Since normal LAEs found in the previous narrow-band imaging surveys are young and low-mass galaxies with a $sSFR \sim 1$–100 Gyr^{-1}, it turns out that most MAESTLOs have a much lower sSFR (Table 1). Thus we infer that MAESTLOs are in the final stage of massive galaxy formation where their SFRs decrease as gas is ejected from the galaxy either by the superwind or AGN outflow or both. If the sizes in the rest-frame UV continuum represent the stellar mass distribution of MAESTLOs, their sizes are very similar to those of compact massive quiescent galaxies found at $z \sim 2$ (van der Wel et al. 2014), implying that the MAESTLOs can be interpreted as their progenitors. It has been recently suggested that massive compact star-forming galaxies at $z \sim 2$–3 evolve into compact quiescent galaxies after the cease of their star formation (e.g., Barro et al. 2013). Although they are mostly dusty galaxies whose sizes are as small as the MAESTLOs, they have a younger age of $1.1^{+0.2}_{-0.6}$ Gyr and a higher sSFR of 0.3–3 Gyr^{-1} than MAESTLOs (Barro et al. 2014). We therefore suggest that they will evolve to passive galaxies through the MAESTLO phase.

At $2.5 < z < 3.2$, our survey volume corresponds to 1.9×10^7 Mpc^3 and the number density of MAESTLOs is 4.8×10^{-7} Mpc^{-3}. Thus MAESTLOs may have been missed by previous narrow-band surveys, because their survey volume was insufficient even in a survey with powerful instruments such as Subaru/Suprime-Cam (e.g., Ouchi et al. 2008). Using the stellar mass function of galaxies at the same redshift range (Ilbert et al. 2013), we compared the number density of MAESTLOs with star-forming and quiescent galaxies with $M_\star > 10^{10.5}\ M_\odot$ and found that MAESTLOs constitute 0.3–0.7% of star-forming galaxies and $\sim 2\%$ of quiescent galaxies. If we assume that all galaxies with $M_\star > 10^{10.5}\ M_\odot$ pass the phase of MAESTLO when they evolve from star-forming to quiescent galaxies, the duration of this phase is estimated as $\sim 0.02 \times t_{univ}(z \sim 3$–$4) \sim 30$–$50$ Myr, making them a rare population. Such short timescale truncation has been recently discussed based on other observational properties of galaxies at $z \sim 3$ (Durkalec et al. 2015; Mancini et al. 2015).

How the star formation was quenched in high-redshift massive galaxies is now the most important issue for understanding galaxy formation and evolution. Detailed observations of MAESTLOs such as integral field spectroscopy and large volume surveys for such massive galaxies with extremely large EW(Lyα) by, for example, Subaru/Hyper Suprime-Cam will allow us to reveal the physical mechanisms of quenching in massive galaxies in the early universe.

We would like to thank both the Subaru and HST staff for their invaluable help, and all members of the COSMOS team.

We also thank Alex Hagen for kindly providing us with the information of their LAEs. This work was financially supported in part by JSPS (YT: 15340059, 17253001, 19340046, and 23244031; TN: 23654068 and 25707010).

REFERENCES

Barro, G., Faber, S. M., Pérez-González, P. G., et al. 2013, ApJ, 765, 104
Barro, G., Faber, S. M., Pérez-González, P. G., et al. 2014, ApJ, 791, 52
Bouwens, R. J., Illingworth, G. D., Labbe, I., et al. 2011, Nature, 469, 504
Brammer, G. B., van Dokkum, P. G., & Coppi, P. 2008, ApJ, 686, 1503
Bruzual, G., & Charlot, S. 2003, MNRAS, 344, 1000
Calzetti, D., Armus, L., Bohlin, R. C., et al. 2000, ApJ, 533, 682
Capak, P., Aussel, H., Ajiki, M., et al. 2007, ApJS, 172, 99
Chabrier, G. 2003, PASP, 115, 763
Cowie, L. L., Songaila, A., Hu, E. M., & Cohen, J. G. 1996, AJ, 112, 839
Donley, J. L., Koekemoer, A. M., Brusa, M., et al. 2012, ApJ, 748, 142
Durkalec, A., Le Fèvre, O., de la Torre, S., et al. 2015, A&A, 576, L7
Elvis, M., Civano, F., Vignali, C., et al. 2009, ApJS, 184, 158
Finkelstein, S. L., Papovich, C., Dickinson, M., et al. 2013, Nature, 502, 524
Gawiser, E., Francke, H., Lai, K., et al. 2007, ApJ, 671, 278
Hagen, A., Ciardullo, R., Gronwall, C., et al. 2014, ApJ, 786, 59
Hasinger, G., Cappelluti, N., Brunner, H., et al. 2007, ApJS, 172, 29
Ilbert, O., McCracken, H. J., Le Fèvre, O., et al. 2013, A&A, 556, A55
Kauffmann, G., Heckman, T. M., White, S. D. M., et al. 2003, MNRAS, 341, 33
Kennicutt, R. C., Jr. 1998, ARA&A, 36, 189
Koekemoer, A. M., Aussel, H., Calzetti, D., et al. 2007, ApJS, 172, 196
Konno, A., Ouchi, M., Ono, Y., et al. 2014, ApJ, 797, 16
Kunth, D., Mas-Hesse, J. M., Terlevich, E., et al. 1998, A&A, 334, 11
Lai, K., Huang, J.-S., Fazio, G., et al. 2008, ApJ, 674, 70
Mancini, C., Renzini, A., Daddi, E., et al. 2015, MNRAS, 450, 763
McCracken, H. J., Milvang-Jensen, B., Dunlop, J., et al. 2012, A&A, 544, A156
Mori, M., & Umemura, M. 2006, Nature, 440, 644
Nagao, T., Murayama, T., Maiolino, R., et al. 2007, A&A, 468, 877
Nilsson, K. K., Møller, P., Möller, O., et al. 2007, A&A, 471, 71
Ono, Y., Ouchi, M., Mobasher, B., et al. 2012, ApJ, 744, 83
Ono, Y., Ouchi, M., Shimasaku, K., et al. 2010, MNRAS, 402, 1580
Ouchi, M., Shimasaku, K., Akiyama, M., et al. 2008, ApJS, 176, 301
Peng, C. Y., Ho, L. C., Impey, C. D., & Rix, H.-W. 2002, AJ, 124, 266
Peng, Y.-j., Lilly, S. J., Kovač, K., et al. 2010, ApJ, 721, 193
Renzini, A. 2009, MNRAS, 398, L58
Sandberg, A., Guaita, L., Östlin, G., Hayes, M., & Kiaeerad, F. 2015, arXiv:1501.06017
Sanders, D. B., Salvato, M., Aussel, H., et al. 2007, ApJS, 172, 86
Schaerer, D. 2003, A&A, 397, 527
Schenker, M. A., Ellis, R. S., Konidaris, N. P., & Stark, D. P. 2014, ApJ, 795, 20
Schinnerer, E., Smolčić, V., Carilli, C. L., et al. 2007, ApJS, 172, 46
Schirmer, M., Diaz, R., Holhjem, K., Levenson, N. A., & Winge, C. 2013, ApJ, 763, 60
Scoville, N., Aussel, H., Brusa, M., et al. 2007, ApJS, 172, 1
Shibuya, T., Kashikawa, N., Ota, K., et al. 2012, ApJ, 752, 114
Taniguchi, Y., Kajisawa, M., Kobayashi, M. A. R., et al. 2015, submitted to PASJ
Taniguchi, Y., Scoville, N., Murayama, T., et al. 2007, ApJS, 172, 9
van der Wel, A., Franx, M., van Dokkum, P. G., et al. 2014, ApJ, 788, 28